

Thermal Stability of the Solidlike and Liquidlike Phases of $(C_{60})_n$ Clusters

F. Calvo[†]

DRFMC/SI2A, CEA Grenoble, 17 rue des Martyrs, F38054 Grenoble Cedex, France, and
University Chemical Laboratory, Lensfield Road, Cambridge CB2 1EW, U.K.

Received: October 5, 2000; In Final Form: December 11, 2000

We report extensive simulation results on the finite temperature behavior of small clusters of C_{60} molecules. The interaction between C_{60} molecules is described by a simple all-atom model, as well as the Pacheco-Prates-Ramalho united-atom potential which includes 2- and 3-body terms. We perform parallel tempering Monte Carlo simulations in both the microcanonical and canonical ensembles. By enclosing the clusters into a hard-wall sphere of increasing radius R and by calculating the thermodynamical properties, we are able to distinguish the boiling phase change from the melting phase change in the case of $(C_{60})_7$, but not in the case of $(C_{60})_{13}$. Analyzing the isomers distributions for $n = 7$ shows that the liquidlike state of $(C_{60})_7$ can be unambiguously defined in a range of temperature below 800 K. The influence of the internal degrees of freedom appears to be limited to an extra peak in the heat capacity near 80 K which characterizes the orientational phase change. Finally, we calculate the average kinetic energy release after evaporation from molecular dynamics simulations, and we compare these results with the predictions of the phase space theory (PST) for different values of R . We show that the PST results provide a clear definition of the boiling energy, and confirm that the largest 13-molecule cluster sublimates molecules as soon as it melts.

I. Introduction

The bulk phases of C_{60} have attracted a lot of attention since a reliable method for synthesizing fullerite was proposed a decade ago.¹ From both experimental² and theoretical³ studies, the low-temperature behavior of solid C_{60} is known to exhibit an orientational phase transition. On the other hand, the existence of a liquid phase was still controversial^{4,5} until Caccamo and co-workers⁶ predicted, on the basis of Girifalco's spherical potential,⁷ that the liquid state should be stable in a narrow region on the phase diagram. This prediction has been confirmed recently by Ferreira et al.⁹ using the more accurate Pacheco-Prates-Ramalho (PPR) potential.⁸ Unfortunately, no experimental result has supported this prediction yet.

After the first clusters of C_{60} molecules were produced and analyzed by Martin et al.,¹⁰ several theoretical investigations on the structural^{11,12} and thermodynamical^{14,15} properties of these species were carried out, essentially with means of the Girifalco potential,¹¹ and more recently with all-atom models¹² and the PPR potential.¹³ While small sizes seem to exhibit pentagonal geometries in a way similar to simple van der Waals atomic clusters,¹⁶ the very short range of the intermolecular potential induces a transition toward decahedral shapes as soon as the system grows beyond 13 molecules.^{11,12} This crossover is shifted to 17 if the cluster is described by all-atom models¹² or by the PPR potential.¹³ The short range of the intermolecular potential was also seen to induce sublimation before any liquidlike state could be attained in $(C_{60})_{13}$.¹⁴ Very recently, Gallego and co-workers have investigated by molecular dynamics (MD) simulations the thermodynamical behavior of a smaller cluster, namely $(C_{60})_7$.¹⁵ Surprisingly, they found this cluster to display a clear liquidlike state in a range of energies, characterized by isomer-

izations in the microcanonical ensemble. The interest in temperature effects on the structure and stability of clusters of fullerene molecules has again grown recently with the experimental discovery by Branz et al.¹⁷ of possible thermally induced structural transitions. In particular, these authors have found evidence of both icosahedral and close-packed stable geometries from the greater intensity in the mass spectra, depending on the temperature.¹⁷ Structural transitions have also been reported theoretically by Luo and co-workers using the PPR potential.¹⁸

Theoretical studies on bulk fullerite have made a great use of Monte Carlo (MC) methods to study phase equilibria.⁴ However, up to now, nearly all dynamical calculations on clusters have been obtained with the Girifalco potential, and only MD simulations have been used in the context of phase changes. In the present paper, we address several questions related to the stability of both the solidlike and liquidlike phases of $(C_{60})_n$ clusters. (i) The usual control parameter for the solidlike–liquidlike transition is the temperature rather than the energy, which is also especially experimentally relevant when the clusters are initially in contact with a thermostat. How are the phases and phase changes affected in the canonical ensemble? (ii) Even though Girifalco's potential is expected to be a reasonable approximation to the interaction between C_{60} molecules at high temperatures, the Pacheco-Prates-Ramalho potential obtained from sophisticated density-functional theory (DFT) calculations has been shown to differ significantly from Girifalco's potential, especially at short distances,⁸ giving rise to noticeable differences in the bulk phase diagram.^{8,9} However, any united-atom potential may be not accurate enough as soon as orientational freezing takes place. Clusters as small as 7 molecules may show very smooth phase changes, and it is important to check that such approximations do not influence the thermal behavior at higher temperatures. Therefore a comparison should be made with an all-atom calculation. (iii) Previous works on the Ar_7 cluster have demonstrated that the

[†] Permanent address: Laboratoire de Physique Quantique, IRSAMC, Université Paul Sabatier, 118 Route de Narbonne, F31062 Toulouse Cedex, France. E-mail: florent@irsamc.ups-tlse.fr.

classical dynamics of this system may be non ergodic in a range of energies.¹⁹ In view of the similarities between van der Waals and C_{60} – C_{60} interactions, one can fear that a similar problem occurs for $(C_{60})_7$. Hence it is necessary to use improved methods that correct this possible nonergodicity problem. (iv) The stability of the liquid phase may be hard to investigate by simulation at low energies, because of the long time required for evaporating a molecule. The evaporation or sublimation processes may be investigated using statistical rate theories instead of MD. More generally, a proper study of the stability of the solidlike and liquidlike phases requires different methodologies.

In the present work, the four subjects above are investigated using complementary approaches based on MC and MD simulations. We have used the PPR potential and a simple all-atom model expected to be more realistic at low temperatures. The various methods are briefly presented in the next section. Section III describes and discusses our results for the solidlike–liquidlike phase change of the two clusters containing 7 and 13 C_{60} molecules, respectively. In Section IV, we investigate the evaporation statistics of these clusters and the related stability of the liquidlike phase at low energies. Finally, we summarize our findings and conclude in Section V.

II. Simulation Methods

We have used two classical potentials to describe the interaction between C_{60} molecules. First, an all-atom (AA) model was chosen from the potentials already used for graphite. In this model, the fullerene molecules are considered as rigid bodies, and the energy V_{ij}^{AA} between any two of them is written

$$V_{ij}^{AA} = \sum_{k_i=1}^{60} \sum_{k_j=1}^{60} 4\epsilon_{AA} \left[\left(\frac{\sigma_{AA}}{r_{k_i k_j}} \right)^{12} - \left(\frac{\sigma_{AA}}{r_{k_i k_j}} \right)^6 \right] \quad (1)$$

where the sum is calculated over all k_i atoms of molecule i and all k_j atoms of molecule j . The distance between atoms k_i and k_j has been denoted $r_{k_i k_j}$. The Lennard-Jones (LJ) parameters ϵ_{AA} and σ_{AA} are taken from the work by Girifalco,⁷ namely $\epsilon_{AA} = 33.26$ K and $\sigma_{AA} = 3.47$ Å. Such a potential is the most simple all-atom model that can be used, in principle, in the low-temperature regime. A more accurate description is however needed to stabilize the $Pa\bar{3}$ crystalline structure, and several groups have made improvements by including partial charges and electrostatic interactions.²⁰ These improved potentials have been tested only on bulk properties, and therefore there is no real need to use them in the present work on finite systems. Furthermore, even in this form, the AA potential remains numerically demanding for statistical purposes.

The most common approximation to the intermolecular potential between C_{60} molecules at reasonably high temperatures is Girifalco's spherical potential,⁷ which consists of summing the contributions of LJ centers homogeneously distributed on the surfaces of the two molecules. This approximation should be valid when the C_{60} molecules are able to rotate freely in space, but without deforming too much. Extensions of Girifalco's original idea have been made to treat the interaction between carbon nanotubes and buckyballs.²¹ Recently, Pacheco and Prates-Ramalho have proposed a more accurate potential for describing the interaction between two and several fullerene molecules.⁸ Their calculations are based on the local density approximation (LDA) of DFT, and include the first-principle computation of the dispersion interaction energy from time-dependent DFT. The total PPR potential is written

$$V_{PPR}(\mathbf{R}) = \sum_{i < j} V_{2body}(r_{ij}) + \sum_{i < j < k} V_{3body}(r_{ij}, r_{jk}, r_{ik}) \quad (2)$$

The 2-body interaction term is expressed as

$$V_{2body}(r) = F(r) \times M(r) + [1 - F(r)] \times W(r) \quad (3)$$

with $M(r) = M_0 \exp[\tau(1 - r/d_0)]\{\exp[\tau(1 - r/d_0)] - 2\}$, a Morse potential acting as the short-range repulsion, and $W(r) = -C_6/r^6 - C_8/r^8 - C_{10}/r^{10} - C_{12}/r^{12}$ the long-range attractive van der Waals expansion. The crossover of these two regimes is described by a Fermi function $F(r) = \{1 + \exp[(r - \mu)/\delta]\}^{-1}$. The 3-body interaction term is the usual triple-dipole Axilrod-Teller potential

$$V_{3body}(r_{ij}, r_{jk}, r_{ik}) = C_{AT} \sum_{i < j < k} \frac{1 + 3 \cos \hat{ijk} \cos \hat{jik} \cos \hat{kji}}{(r_{ij} r_{jk} r_{ik})^3} \quad (4)$$

The parameters of the PPR potential are given in Table 1.

To investigate the change from the solidlike phase to the fluidlike phase, we have chosen Monte Carlo methods rather than molecular dynamics. This choice was motivated by the need of a high statistical accuracy, but also by the possible problem of nonergodicity at low energies met by MD simulations, especially for the smaller 7-molecule cluster.¹⁹ To accelerate convergence and overcome quasi-ergodicity, we have employed the parallel tempering (PT) technique.^{22–24} This method consists of performing simultaneously the various trajectories at different temperatures, allowing occasional exchanges between configurations of adjacent trajectories. It has been successfully used in simulations of complex systems in the past,^{22–27} and more recently for clusters exhibiting a slow interfunnel relaxation such as the 38-atom LJ cluster.^{28,29} We just recall here the principle of a PTMC simulation in the canonical ensemble. Let $\{T_i = 1/k_B \beta_i\}$ be a set of M different temperatures at which we want to sample the equilibrium properties of our system characterized by its potential energy $V(\mathbf{R})$ at configuration \mathbf{R} . With probability χ , all M trajectories are propagated as usual, by randomly displacing configurations from $\mathbf{R}_i^{\text{old}}$ to $\mathbf{R}_i^{\text{new}}$. In the Metropolis scheme, the new configuration $\mathbf{R}_i^{\text{new}}$ is accepted with the probability

$$\text{acc}(\mathbf{R}_i^{\text{old}} \rightarrow \mathbf{R}_i^{\text{new}}) = \min\{1, \exp[-\beta_i(V(\mathbf{R}_i^{\text{new}}) - V(\mathbf{R}_i^{\text{old}}))]\} \quad (5)$$

With probability $1 - \chi$, an exchange is attempted between the configurations of trajectories i and $j = i + 1$ chosen randomly. This exchange is accepted with the probability

$$\text{acc}(\mathbf{R}_i \rightleftharpoons \mathbf{R}_j) = \min\{1, \exp[\Delta\beta\Delta V]\} \quad (6)$$

where $\Delta\beta = \beta_i - \beta_j$ and $\Delta V = V(\mathbf{R}_i) - V(\mathbf{R}_j)$. This acceptance probability ensures that detailed balance is satisfied, hence that the MC process is Markovian.

To compare our results to those obtained by Gallego and co-workers,¹⁵ we have also performed PTMC simulations in the molecular dynamics ensemble. These simulations only differ from the standard (canonical) PTMC simulations by the laws governing the acceptance probabilities of attempting Monte Carlo moves or parallel tempering exchanges. The molecular dynamics ensemble is the ensemble effectively sampled from classical isoergic MD simulations. It is similar to the microcanonical ensemble except that it incorporates the two additional mechanical constraints on the total linear and angular momenta. For atomic systems, it can be shown that the probability of

TABLE 1: Parameters of the Pacheco-Prates-Ramallo United-Atom Potential, Taken from Ref 8

C_6 (eV/Å ⁶)	C_8 (eV/Å ⁻⁸)	C_{10} (eV/Å ⁻¹⁰)	C_{12} (eV/Å ⁻¹²)	M_0 (eV)	τ	d_0 (Å)	μ (Å)	δ (Å)	C_{AT} (eV/Å ⁻⁹)
7.56×10^4	9.1224×10^6	2.09×10^8	7.78×10^{10}	0.3	9.75	10.3	10.05	1.04	4.752×10^6

attempting a MC move from configuration $\mathbf{R}_i^{\text{old}}$ toward $\mathbf{R}_i^{\text{new}}$ at total energy E_i should now read²⁹

$$\text{acc}(\mathbf{R}_i^{\text{old}} \rightarrow \mathbf{R}_i^{\text{new}}) = \min \left\{ 1, \left[\frac{E_i - V(\mathbf{R}_i^{\text{new}})}{E_i - V(\mathbf{R}_i^{\text{old}})} \right]^s \times \left(\frac{\det \mathbf{I}(\mathbf{R}_i^{\text{old}})}{\det \mathbf{I}(\mathbf{R}_i^{\text{new}})} \right)^{1/2} \Theta[E_i - V(\mathbf{R}_i^{\text{new}})] \right\} \quad (7)$$

with the exponent $s = 3N/2 - 4$ for N pseudo-atoms, and Θ the Heaviside step function: $\Theta(x) = 1$ if $x \geq 0$, $\Theta(x) = 0$ otherwise. The inertia matrices $\mathbf{I}(\mathbf{R}_i^{\text{old}})$ and $\mathbf{I}(\mathbf{R}_i^{\text{new}})$ enter this expression as the result of the conservation of angular momentum.³⁰

In the MD ensemble, a parallel tempering exchange between configurations \mathbf{R}_i and \mathbf{R}_j initially in trajectories at total energies E_i and E_j , respectively, is accepted with probability²⁹

$$\text{acc}(\mathbf{R}_i \rightleftharpoons \mathbf{R}_j) = \min \left\{ 1, \left[\frac{(E_i - V(\mathbf{R}_j))(E_j - V(\mathbf{R}_i))}{(E_i - V(\mathbf{R}_i))(E_j - V(\mathbf{R}_j))} \right]^s \right\} \quad (8)$$

provided that all quantities inside brackets are positive. In the canonical ensemble, PTMC simulations were carried out with the two potentials, and the quaternion coordinates were used to describe the internal degrees of freedom in the all-atom model. Only the pseudo-atom potential was used for the PTMC simulations in the MD ensemble. In both cases, the caloric curves (heat capacities) were calculated by a multiple-histogram analysis of the distribution of configurational energies from all trajectories.

III. Thermodynamics of Melting

At finite temperature, the lowest free-energy minimum of a free finite system is not the condensed phase, but the vapor.³¹ Simulating cluster melting at equilibrium thus requires us to enclose the system into a repulsive container in order to prevent evaporation.³² However, the caloric curves are known to be somewhat dependent on the volume or the radius of the available configuration space.^{33,34} Indeed, too small a radius would create an external pressure which affects essentially the solidlike, while too large a radius leads to many evaporation events and a possible precursor to the boiling transition.³⁴

In the case of $(C_{60})_n$ clusters, we expect evaporation to be easier than in the case of LJ_n clusters, in particular since it tends to become sublimation. In this respect, the possibility of varying the size of the container appears to be a sensitive probe of the different phase changes. We have used a simple hard-wall spherical wall, which is most convenient in MC simulations, and we have chosen two different radii for each size, namely $R = 15$ Å and 40 Å for $(C_{60})_7$, and $R = 20$ Å and 50 Å for $(C_{60})_{13}$.

All simulations using the PPR potential consisted of 10^6 MC sweeps, one sweep being N individual MC steps. The equilibration time was taken as 2×10^5 sweeps. With the all-atom potential, we only studied the smallest cluster, with 5×10^5 sweeps following 10^5 equilibration sweeps. Parallel tempering exchanges were attempted with 10% probability. From the histogram analysis, the microcanonical entropy $S(E)$ was computed, and the microcanonical heat capacities was calculated as $C_\mu(E) = \partial E / \partial T_\mu$ where $T_\mu(E) = \partial S / \partial E$ is the microcanonical

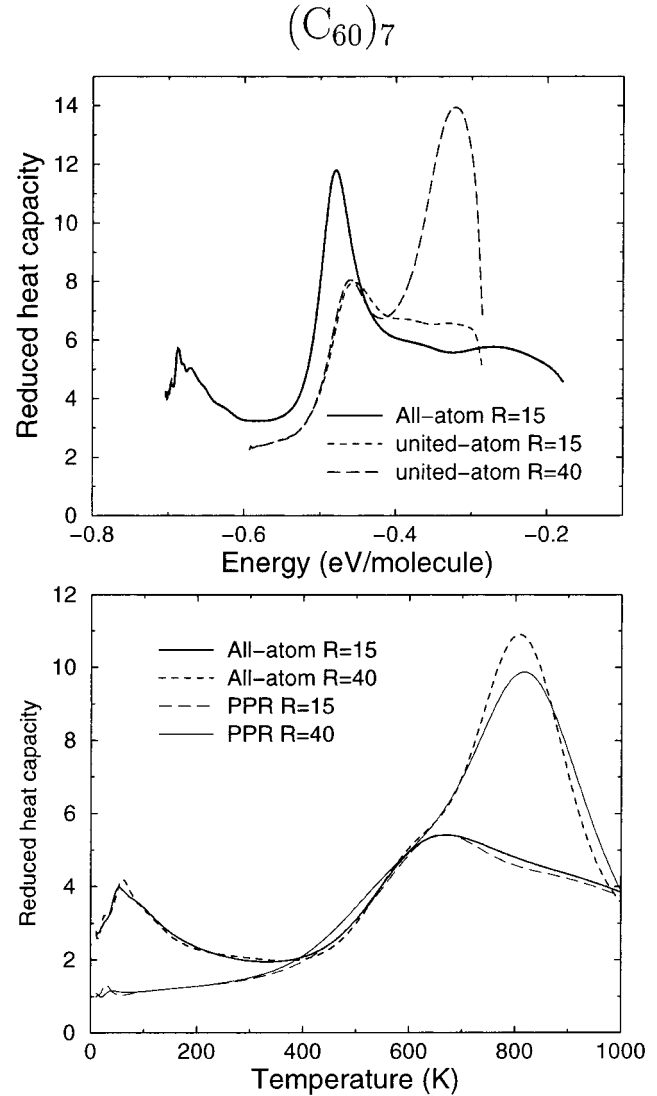


Figure 1. Heat capacity of the $(C_{60})_7$ cluster for various radii of the container, and for both the united-atom and all-atom potentials. Upper panel: results in the microcanonical ensemble; lower panel: results in the canonical ensemble.

temperature. The canonical heat capacity at constant volume is $C_v(T) = \partial U / \partial T = [\langle E^2 \rangle - \langle E \rangle^2] / k_B T^2$, the average being canonical.

We have represented in Figure 1 the heat capacities for the smallest cluster containing 7 molecules. In the microcanonical ensemble, the curves calculated with the PPR potential agree with the direct MD simulations of Gallego and co-workers using the Girifalco potential,¹⁵ but they are slightly shifted to higher energies. An extra peak appears at high energies for large containers, but the curve is not affected below -0.4 eV/molecule. The curve calculated with the all-atom potential is in reasonable agreement with the PPR potential, however there is an extra peak at low energy, which is also present for larger radii of the container. In this case, the high-energy region also shows some peaks above -0.4 eV/molecule, but we did not plot the corresponding caloric curve to seek clarity. A similar behavior is observed in the canonical ensemble on the lower panel of Figure 1. Here the agreement between the predictions

of the two potentials is very good for both radii above around 400 K. The low-temperature peak occurring near 80 K with the all-atom model can be interpreted as the signature of the orientational phase change.³⁵ For the small radius, the curves display a clear bump near 700 K characteristic of isomerization. However, for the larger radius, the bump is shifted to higher temperatures (~ 800 K) and higher latent heats. Only a small shoulder remains near 700 K. The microscopic analysis has been performed by periodically quenching the cluster along the MC simulation, and by identifying the isomers among the 4 existing stable geometries. In the case of the all-atom model, the quenches were performed with the PPR potential to save computational time. The four isomers, in order of decreasing binding energy, are, respectively, the pentagonal bipyramid (PBP), the capped octahedron (OCT + 1), the incomplete stellated tetrahedron (IST), and the "skew" isomer.³⁶ In addition, we have distinguished the case of dissociated structures where one atom is distant from the cluster center of mass by more than 12 Å. The probability distributions of the five "isomers" in the simulation with radius 40 Å are depicted in Figure 2, for PPR simulations in the microcanonical ensemble, and for all-atom simulations in the canonical ensemble. Because we used parallel tempering, we hope that our simulations have been able to overcome the quasi-ergodic behavior reported earlier on the LJ₇ system.¹⁹ From Figure 2, one can see that isomerization starts near -0.5 eV/molecule, and culminates (i.e., the fraction of the PBP isomer gets below 50%) near the same energy as the microcanonical heat capacity peak, namely at -0.45 eV/molecule. At this energy, dissociation is still a rare event, so we can actually consider the phase as "liquidlike." As energy increases, the ratio of evaporated or fragmented clusters increases too, and goes beyond 50% at the energy -0.3 eV/molecule. This provides us a first estimate of the boiling energy for this cluster, and with the range in which we can consider the liquidlike phase as stable. A qualitatively similar behavior is observed with the all-atom model in the canonical ensemble. Again, the peak in the low-radius heat capacities coincides with the temperature where the PBP isomers becomes less probable than 50%, and the high temperature peak for large radius coincides with the increase of the probability of dissociating above 50%. Thus, we can roughly estimate that the canonical range of stability for the liquidlike phase of (C₆₀)₇ is located between 600 K and 800 K.

The 13-molecule cluster displays rather different thermodynamics. We have represented in Figure 3 the heat capacities obtained with the PPR potential for the two radii $R = 20$ Å and 50 Å, in the microcanonical and canonical ensembles. In the two ensembles, the curves are singly peaked for $R = 20$ Å around the melting energy -0.54 eV/molecule, or the melting temperature 820 K. When the size of the container is large enough to allow for evaporations, the canonical peak rises but does not shift to higher temperatures. Nevertheless, in the microcanonical ensemble, extra peaks appear on the high-energy side. It is not convenient to distinguish the numerous isomers of (C₆₀)₁₃, even for the PPR potential and by partitioning these isomers into separate classes. Instead, we have calculated the phase-space average of the number of fragments inside the spherical hard wall. For this we define a fragment as a set of connected molecules, and a molecule is said to be connected if there exists another molecule located at a distance between centers of mass shorter than 12 Å. The number of fragments as a function of total energy is plotted in Figure 4. The variations observed for the two values of the container radius show a strong rise at the melting energy. Therefore, the boiling phase change

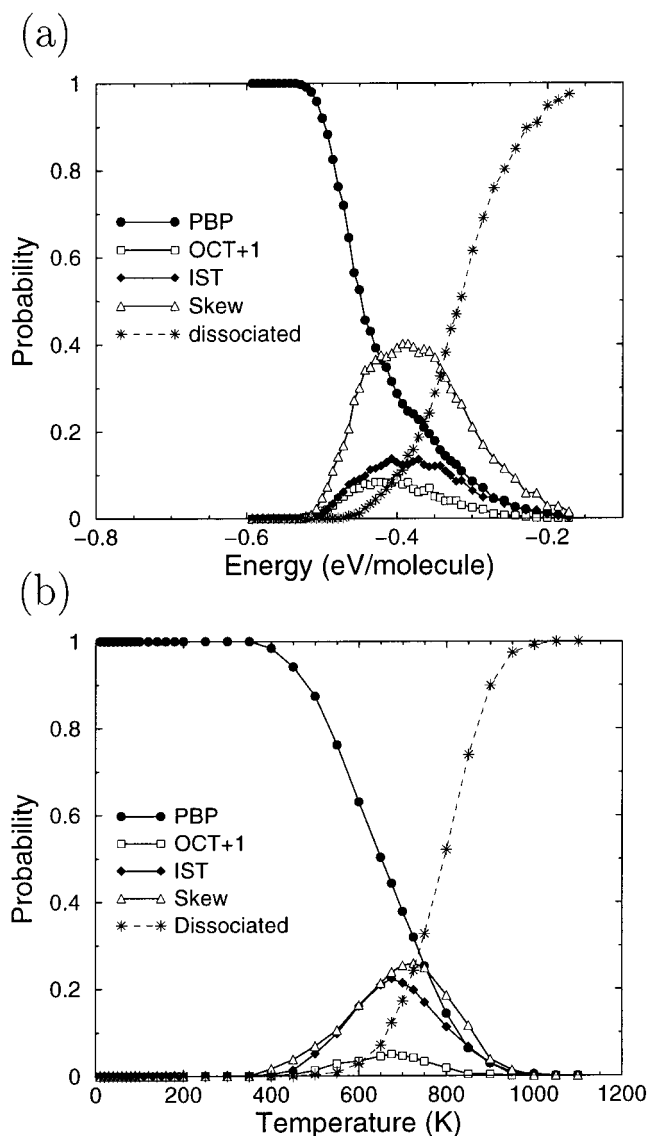


Figure 2. Relative probabilities of finding a particular isomer (pentagonal bipyramid PBP, capped octahedron OCT + 1, incomplete stellated tetrahedron IST, and "skew") or a dissociated geometry in Monte Carlo simulations of (C₆₀)₇ with container radius $R = 40$ Å. (a) United-atom potential in the microcanonical ensemble; (b) All-atom model in the canonical ensemble.

seems to take place as soon as melting occurs. This sublimation process is consistent with the previous observations by Gallego and co-workers¹⁴ although these authors did not consider the boiling transition in itself. We now discuss the evaporation phenomenon on a more quantitative basis.

IV. Evaporation Statistics

The results presented in the previous section have shown that it can be hard to distinguish the melting phase change from boiling in (C₆₀)_n clusters as soon as the enclosing radius gets large. Indeed, in vacuum, the stability of an isolated cluster above its melting point should be discussed in terms of time scales, or evaporation rates. In this case, a "hot" cluster will be considered stable if it has not evaporated molecules within the typical observation time. Here we consider the thermal stability of the liquidlike phase more specifically, by investigating the statistics of unimolecular evaporation, and by focusing in particular on the average kinetic energy release. In the following, all calculations have been made using the united-atom PPR

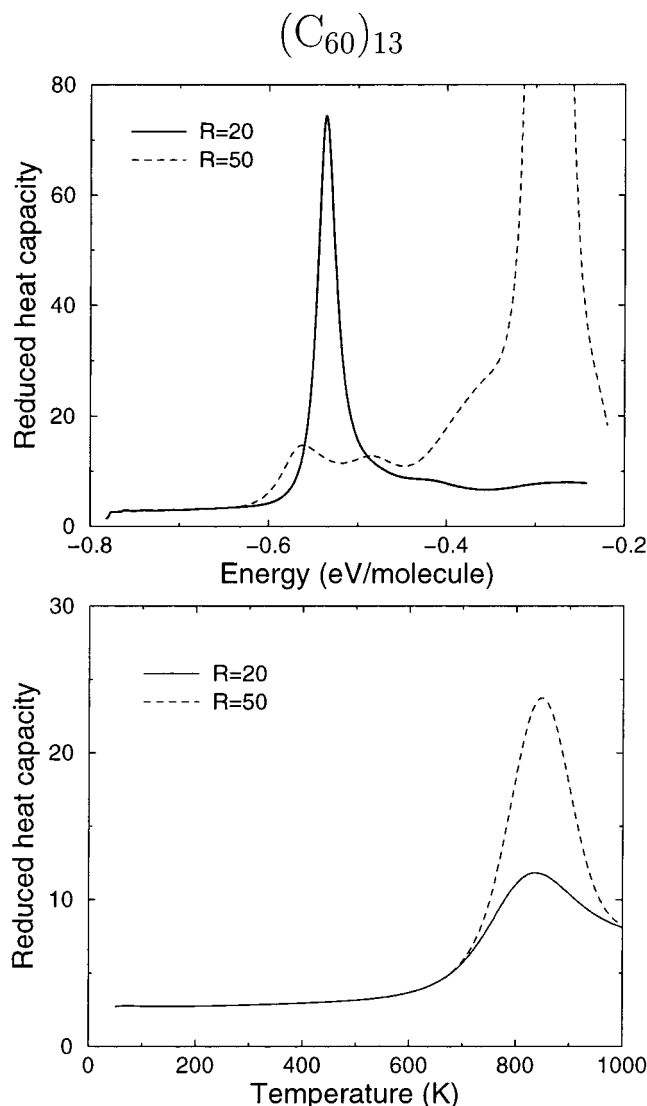


Figure 3. Heat capacity of $(C_{60})_{13}$ in the united-atom PPR model, for the two containers $R = 20$ Å and $R = 50$ Å. Upper panel: microcanonical ensemble; lower panel: canonical ensemble.

potential, so that we neglect the effects of the internal orientational degrees of freedom of the molecules.

There have been several theoretical and computational works on the evaporation of weakly bound clusters in the past,³⁷ but the most notable advance was due to Weerasinghe and Amar³⁸ who compared the results of brute force MD simulations to the predictions of several statistical rate theories. We follow similar lines here, with the restriction that we are interested mostly in the average kinetic energy release, but not in the (absolute) evaporation rates. First, we have simulated the cluster evaporation in the same way as in refs 37, 38. Briefly, a low-temperature sample of starting configurations is created, and each configuration is heated to a given total energy and with zero angular momentum. As soon as an atom has dissociated (see the definition of a connected atom in the previous section), one records the lifetime of the reactant cluster and the total kinetic energy (translational plus rotational) released in the evaporation process. By recording the number $N(t)$ of clusters having survived after time t , the logarithmic plot of N versus t yields a straight line characteristic of unimolecular processes.

The data obtained by direct simulations has been compared with the predictions of the same three statistical theories as previously investigated by Weerasinghe and Amar.³⁸ We will

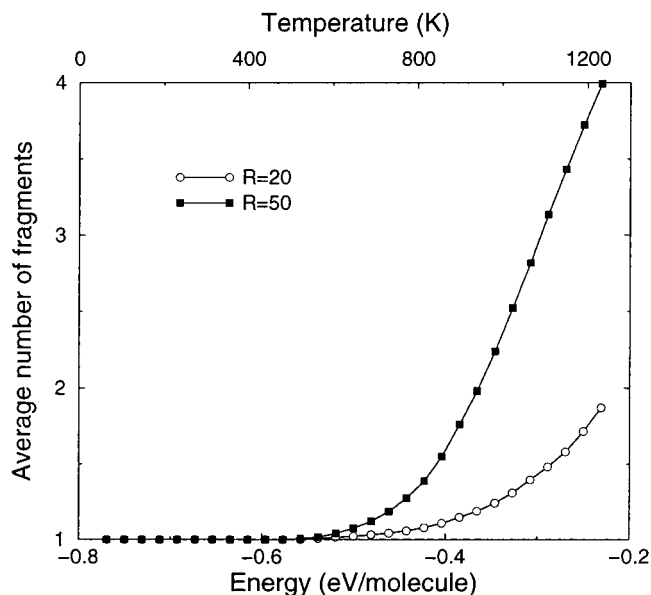


Figure 4. Statistical average of the number of fragments of $(C_{60})_{13}$ inside the container $R = 50$ Å from Monte Carlo simulation in the microcanonical ensemble. See the text for the definition of a fragment. An indicative temperature scale is also given on the upper abscissa axis.

not address these theories in details here, and we refer the reader to ref 38 for a more complete treatment.

In the Rice-Ramsperger-Kassel (RRK) theory,³⁹ the n -atom system is considered as a collection of $\nu = 3n - 6$ identical harmonic oscillators. The classical expression for the average kinetic energy release $\langle\epsilon\rangle$ as a function of total energy E in the reactant cluster is expressed as

$$\langle\epsilon\rangle_{\text{RRK}}(E) = (E - D_0)/\nu \quad (9)$$

where D_0 is the energy of the transition state. Assuming that evaporation is a barrierless process (loose transition state approximation), D_0 is also the energy difference between the most stable configurations of the reactant and product clusters.

In the Engelking or Weisskopf theories,⁴⁰ the angular momentum conservation and microscopic reversibility are taken into account and the expression for $\langle\epsilon\rangle$ becomes

$$\langle\epsilon\rangle_{\text{Engelking}}(E) = 2(E - D_0)/(\nu - 1) \quad (10)$$

The phase space theory (PST), as formulated by Chesnavitch and Bowers,⁴¹ does not make use of the harmonic approximation in the vibrational densities of states (DOS). Following a recent work on aniline- Ar_n clusters,⁴² one can simplify the rotational densities of states, and give an expression for the average kinetic energy release in terms of the anharmonic DOS of the product cluster only:

$$\langle\epsilon\rangle_{\text{PST}}(E) \approx \frac{\int_0^{E-D_0} \epsilon^2 \omega_{n-1}(E - D_0 - \epsilon) d\epsilon}{\int_0^{E-D_0} \epsilon \omega_{n-1}(E - D_0 - \epsilon) d\epsilon} \quad (11)$$

The evaluation of evaporation rates also requires the knowledge of the vibrational density of states ω_n of the reactant cluster. To compute the PST prediction, we performed additional MC simulations for $(C_{60})_6$ and $(C_{60})_{12}$ bound by the PPR potential, enclosed in spherical containers with the same radii as those used for the reactant sizes. These MC simulations provided, via the histogram reweighting method, the anharmonic vibra-

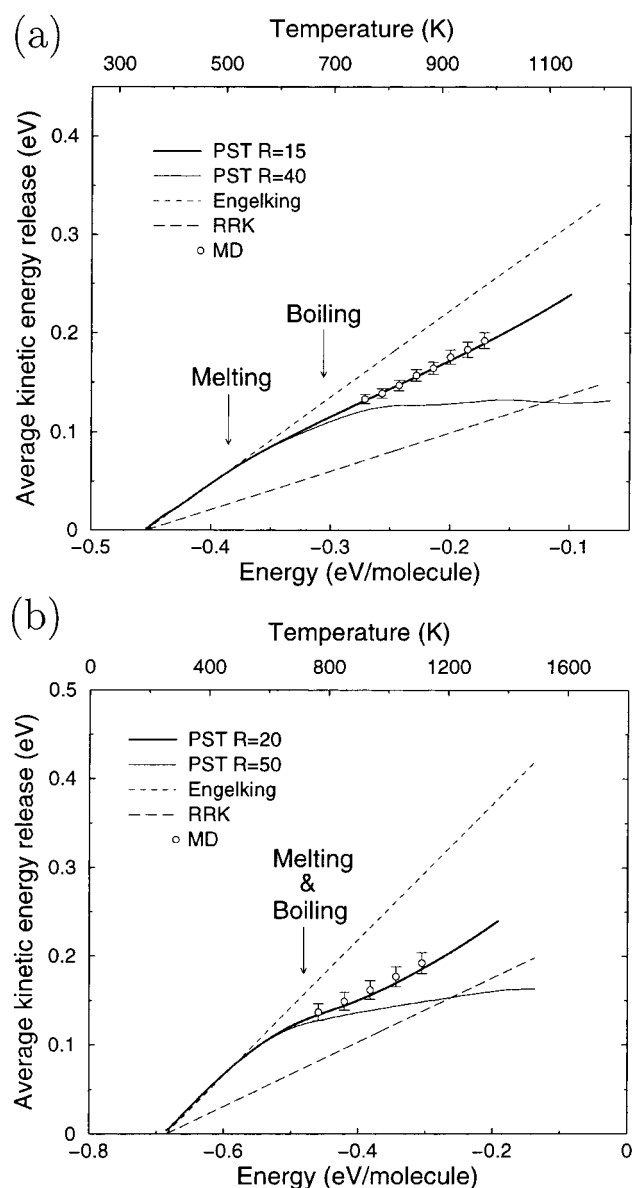


Figure 5. Average kinetic energy released in the unimolecular evaporation process. The continuous lines are the RRK, Engelking, and PST predictions (see text), and the circles are obtained from MD simulations. The melting and boiling energies are indicated by arrows. (a) Results for $(C_{60})_7$; (b) Results for $(C_{60})_{13}$. An indicative temperature scale is also given on the upper abscissa axes.

tional densities of states ω_{n-1} for the two product clusters. The results of the brute force MD simulations and the comparison with the statistical theories are given in Figure 5 for the two sizes $n = 7$ and $n = 13$.

As first noted by Weerasinghe and Amar,³⁸ the “exact” MD results fall between the RRK value which underestimates $\langle \epsilon \rangle$, and the Engelking value which is an overestimate. Only the PST value for the small radius is in very good agreement with MD, also similar to what has been observed in argon clusters. However, there is a divergence in the PST predictions when the density of states is calculated for a large container. This divergence occurs near -0.3 eV/molecule for $(C_{60})_7$ and near -0.5 eV/molecule for $(C_{60})_{13}$. We interpret this disagreement with the MD data as the fact that the calculated DOS do not represent the product clusters in bound, compact configurations. Instead, in these ranges of energies, the product clusters also have evaporated molecules, as can be seen from Figure 4 in the case of $(C_{60})_{13}$. Therefore, the corresponding PST curves

cannot be really considered as representative of the unimolecular evaporation process. This result calls two remarks. First, the sensitivity of the PST calculation with respect to the radius of the container suggests that the MD results could also be sensitive on this parameter. Indeed, taking a large radius for detecting evaporation would be meaningless because of multiple evaporations. We have checked that increasing the radius by 20% resulted only in a shift in the observed evaporation time, but in very small decreases of $\langle \epsilon \rangle$.

Our second remark concerns the unimolecular character of the evaporation process. The large ability of the clusters to evaporate molecules at high energies suggests that this unimolecular hypothesis may not be satisfied in the present case, which would cause the PST to be meaningless. We have also looked for secondary evaporations, and we calculated from molecular dynamics the average times of successive evaporations $t_i(E)$, $i = 1, 2, \dots$ for various total energies. In the range of energies considered for the MD simulations of Figure 5, the average relative time $(t_2 - t_1)/t_1$ was always observed to be larger than 50%. Hence we can safely consider the phase space theory treatment to be valid in the present case.

Now, we have indicated in Figure 5 the melting and boiling energies estimated in the previous section from purely thermodynamical considerations for the two clusters. In both cases, the divergence of the PST curves for small and large radii of the container occurs at (or close to) the boiling energy. Because the PST data was obtained from simulation of the *product* clusters, this result is fully independent from the thermodynamics of the *reactant* cluster. In fact, we think that it provides an alternative, unambiguous way for defining boiling points in finite systems. From the picture of Figure 5, we see what makes the difference between the thermal behavior of $(C_{60})_7$ and $(C_{60})_{13}$ at high energies. In particular, we can now clearly state that, while the small 7-molecule cluster displays a rather stable liquidlike state, the icosahedral 13-molecule cluster sublimates molecules as soon as it melts. This result could lead us think that only the very small clusters of fullerene molecules can have a stable liquidlike phase in isolated form. However, clusters are usually capable of exhibiting a very rich variety of size effects, especially prior to melting.⁴³ Therefore, we believe that the present conclusions on $(C_{60})_{13}$ should not be extended to all sizes above 13, even though it is most probable that only a few specific sizes may have a reasonable large range of stability in the liquidlike region. As one gets closer to the thermodynamic limit, pressure effects help to stabilize the liquid phase. In some way, the presence of a container mimics these effects for small clusters.

The instability of the liquidlike phase of $(C_{60})_{13}$ results from the rather large energy needed to extract a molecule from the icosahedral surface, while rearranging $(C_{60})_7$ requires comparatively less energy. Removing or adding a molecule to the 13-molecule system could yield some premelting phase where either the vacancy or the floater could move (or hop) freely on the surface.⁴⁴ More generally, we can expect the phase diagram $T_{\text{melting}}(n) \leq T \leq T_{\text{boiling}}(n)$ to exhibit a strong size-dependence up to the regime where volume melting becomes the dominant process.

V. Discussion and Conclusions

The properties of clusters of fullerene molecules are unusual owing to the very short range of the intermolecular potential.⁴⁵ We have investigated the finite-temperature behavior of two such clusters, containing, respectively, 7 and 13 molecules. Because the condensed disordered phase may not be stable in

a wide range of energies or temperatures, the use of a container was necessary to prevent evaporation. Indeed, the radius of this container appears to be a suitable parameter for getting insight into the boiling phase change, thus confirming previous works by Tsai and Jordan³³ and by Moseler and Nordiek.³⁴ The thermal equilibrium of $(C_{60})_n$ clusters in the canonical ensemble is relevant only in the presence of this container, otherwise the vapor would be more stable for $T > 0$. By enclosing the clusters into this container, we have been able to study the actual phases and phase changes of these clusters by finding observables that are appropriate to either the solidlike, the liquidlike, or the vapor phases.

The stability of the solidlike phase is relatively easy to work out, because one can quite safely identify the corresponding unique isomer. We could estimate the upper limit of stability of the solidlike phase by quenching the cluster and by finding it in the global minimum more than 50% of the time. This point was illustrated in details in the case of $(C_{60})_7$, but could be extended to any other size. For this, we could for instance consider all compact isomers except the ground state as forming the disordered phase. Nevertheless, such studies would be irrelevant in the case of structural transitions occurring below the melting temperature.

This work shows a good agreement between the results obtained by Gallego and co-workers¹⁵ with the simple Girifalco spherical potential and the present results using the more accurate Pacheco-Prates-Ramalho united-atom potential. The situation is a bit more complicated for all-atom models, for which calculations have shown that the real solid phase exists only up to around 80 K. Above this temperature, orientational melting occurs, and the molecules become hot enough to undergo free rotation around their centers of mass. Even though this transition occurs at a higher temperature (≈ 260 K) and is sharp in bulk C_{60} , we have seen that it is smeared out over a wide temperature range for the 7-molecule cluster. The smearing of the caloric curve induced by these molecular properties reaches relatively high temperatures. Thus, so far as thermodynamics is concerned, united-atom potentials such as Girifalco or PPR appear as a reasonable approximation for describing $(C_{60})_7$ only for temperatures larger than around 400 K. Previous studies on the thermal behavior of molecular clusters⁴⁶ have shown that the width of the heat capacity peak associated with orientational freezing tends to get narrower as size increases, as can be expected from a first-order transition rounded by size effects. Therefore, the PPR (and Girifalco) approximations should become more relevant for larger sizes as soon as the temperature gets over 100–150 K. Of course, we are aware that several more realistic intermolecular potentials are available, including electrostatic components, but we believe that the present results would not be quantitatively much affected. Also, we did not consider the possible role of the internal degrees of freedom. At temperatures below 1000 K, only vibrations are expected to occur,⁴⁷ therefore the rigid-molecule approximation is at least qualitatively correct. However, in the same way as the Girifalco is an approximation to the full-site all-atom potential, it would be interesting to have a quantitative estimate of the effect of internal vibrations on the melting process in these clusters.

While it is quite easy to define unambiguously the stability range of the solidlike phase for $(C_{60})_n$ clusters, some problems arise when dealing with the liquidlike phase. Preventing evaporation by using a small container yields heat capacity peaks that can be interpreted as the signature of the solidlike–liquidlike phase change. The strong variations occurring upon

increasing the size of this container show that the liquidlike phase is actually stable only in a narrow temperature range, and only for the smallest cluster. In the canonical ensemble, rough estimates of the upper limit for stability can be obtained by looking at the changes in the caloric curves as the container gets larger. It is also possible to have an estimate from the probability of finding the cluster in a dissociated form. However, in the canonical ensemble, the finite temperature states are bound to decay into vapor after some time.

In the (more relevant) microcanonical ensemble, the liquidlike phase can also be unstable by evaporating molecules, provided that the observation time is long enough at a given total energy. We studied the evaporation process in more quantitative details by calculating the average kinetic energy release from a statistical set of MD simulations, and by comparing these results to the predictions of several rate theories of unimolecular dissociation. Similar to observations by Weerasinghe and Amar,³⁸ the Engelking and RRR values are, respectively, upper and lower bounds for the real data from molecular dynamics. On the other hand, the agreement found with phase space theory strongly depends on the container radius chosen to enclose the product cluster, and is good for small radii only. Taking too large a radius is not relevant as soon as the product cluster itself dissociates, since the hypothesis of unimolecular evaporation of the reactant cluster breaks down. This observation was supported by the calculation of the average number of fragments at equilibrium, which shows a strong rise as the onset of boiling. Actually, the divergence of the PST result allowed us to propose an independent definition of the boiling energy which marks the upper limit of the liquidlike phase. This definition agrees well with other evaluations from caloric or fragmentation studies, but is more robust and can be extended to any size, and other systems for which the loose transition state assumption within the PST is relevant.

The internal structure of C_{60} molecules was seen to have important consequences on the thermodynamical curves of $(C_{60})_n$ clusters, and one may ask whether there would also be changes in the evaporation processes. MD simulations are always possible (although they require a heavy computational effort), however statistical rate theories are still lacking. They should include the rotational contribution to the kinetic energy before and after the dissociation, which requires a proper calculation of the full microcanonical density of states, and especially a reformulation of phase space theory. These points lie beyond the scope of the present paper, but should be addressed in future investigations.

In view of the recent experimental results obtained by the Martin group,¹⁷ it would be interesting to apply the methods used in this work to larger sizes which exhibit structural phase transitions such as 38 or 48. Such studies have now become possible with the use of ergodic sampling methods such as parallel tempering.^{28,29} The specific stability of some sizes against evaporation is what is experimentally measured in the mass spectra obtained from molecular beams. The point of view developed in the present study was more involved in comparing cluster and bulk thermal behaviors. However, it could be extended to larger sizes in an effort to provide a more complete interpretation to the intriguing experimental observations of structural transitions in clusters of fullerene molecules.

Acknowledgment. The author thanks Dr. P. Parneix for very useful discussions.

References and Notes

- (1) Krätschmer, W.; Lamb, L. D.; Fostiropoulos, K.; Huffman, D. R. *Nature (London)* **1990**, 347, 354.

- (2) David, W. I. F.; Ibberson, R. M.; Dennis, T. J. S.; Hare, J. P.; Prassides, K. *Europhys. Lett.* **1992**, *18*, 219; Blaschko, O.; Krexner, G.; Maier, Ch.; Karawatzki, R. *Phys. Rev. B* **1997**, *56*, 2288.
- (3) Cheng, A.; Klein, M. L. *Phys. Rev. B* **1992**, *45*, 1889; Schelkacheva, T. I.; Tareyeva, E. E. *Phys. Rev. B* **2000**, *61*, 3143.
- (4) Hagen, M. H. J.; Meijer, H. J.; Mooij, G. C. A. M.; Frenkel, D.; Lekkerkerker, H. N. W. *Nature (London)* **1993**, *365*, 425.
- (5) Cheng, A.; Klein, M. L.; Caccamo, C. *Phys. Rev. Lett.* **1993**, *71*, 1200.
- (6) Caccamo, C.; Costa, D.; Fucile, A. *J. Chem. Phys.* **1997**, *106*, 255.
- (7) Girifalco, L. A. *J. Phys. Chem.* **1992**, *96*, 858.
- (8) Pacheco, J. M.; Prates-Ramalho, J. P. *Phys. Rev. Lett.* **1997**, *79*, 3873.
- (9) Ferreira, A. L. C.; Pacheco, J. M.; Prates-Ramalho, J. P. *J. Chem. Phys.* **2000**, *113*, 738.
- (10) Martin, T. P.; Näher, U.; Schaber, H.; Zimmermann, U. *Phys. Rev. Lett.* **1993**, *70*, 3079.
- (11) Wales, D. J. *J. Chem. Soc. Faraday Trans.* **1994**, *90*, 1061; Rey, C.; Gallego, L. J.; Alonso, J. A. *Phys. Rev. B* **1994**, *49*, 8491.
- (12) García-Rodeja, J.; Rey, C.; Gallego, L. J. *Phys. Rev. B* **1997**, *56*, 6466; Doye, J. P. K.; Dullweber, A.; Wales, D. J. *Chem. Phys. Lett.* **1997**, *269*, 408.
- (13) Luo, Y.-H.; Zhao, J.; Qiu, S.; Wang, G. *Phys. Rev. B* **1999**, *59*, 14 903.
- (14) Rey, C.; Gallego, L. J.; Alonso, J. A. *Phys. Rev. B* **1994**, *49*, 8491.
- (15) Gallego, L. J.; García-Rodeja, J.; Alemany, M. M. G.; Rey, C. *Phys. Rev. Lett.* **1999**, *83*, 5258.
- (16) Wales, D. J.; Doye, J. P. K. *J. Phys. Chem. A* **1997**, *101*, 5111.
- (17) Branz, W.; Malinowski, N.; Schaber, H.; Martin, T. P. *Chem. Phys. Lett.* **2000**, *328*, 245.
- (18) Zhang, W.; Liu, L.; Zhuang, J.; Li, Y. *Phys. Rev. B* **2000**, *62*, 8276.
- (19) Miller, M. A.; Wales, D. J. *J. Chem. Phys.* **1997**, *107*, 8568.
- (20) Launois, P.; Ravy, S.; Moret, R. *Phys. Rev. B* **1998**, *55*, 2651.
- (21) Girifalco, L. A.; Hodak, M.; Lee, R. S. *Phys. Rev. B* **2000**, *62*, 13 104.
- (22) Swendsen, R. H.; Wang, J.-S. *Phys. Rev. Lett.* **1986**, *57*, 2607.
- (23) Geyer, C. J. In *Computing Science and Statistics: Proceedings of the 23rd Symposium on the Interface*; American Statistical Association: New York, 1991; p 156.
- (24) Marinari, E.; Parisi, G.; Ruiz-Lorenzo, J. In *Spin Glasses and Random Fields*, Vol. 12 of *Directions in Condensed Matter Physics*; Young, A., Ed.; World Scientific: Singapore, 1998.
- (25) Falcioni, M.; Deem, M. W. *J. Chem. Phys.* **1999**, *110*, 1754.
- (26) Yan, Q.; De Pablo, J. J. *J. Chem. Phys.* **1999**, *111*, 9509.
- (27) Cerovski, V. Z.; Mahanti, S. D.; Khanna, S. N. *Euro. Phys. J. D* **2000**, *10*, 119.
- (28) Neirotti, J. P.; Calvo, F.; Freeman, D. L.; Doll, J. D. *J. Chem. Phys.* **2000**, *112*, 10 340.
- (29) Calvo, F.; Neirotti, J. P.; Freeman, D. L.; Doll, J. D. *J. Chem. Phys.* **2000**, *112*, 10 350.
- (30) Calvo, F.; Labastie, P. *Euro. Phys. J. D* **1998**, *3*, 229.
- (31) Lee, J. K.; Barker, J. A.; Abraham, F. F. *J. Chem. Phys.* **1973**, *58*, 3155.
- (32) Labastie, P.; Whetten, R. L. *Phys. Rev. Lett.* **1990**, *65*, 1567.
- (33) Tsai, C. J.; Jordan, K. D. *J. Chem. Phys.* **1993**, *99*, 6957.
- (34) Moseler, M.; Nordiek, J. *Phys. Rev. B* **1999**, *60*, 11 734.
- (35) Maillet, J. B.; Boutin, A.; Fuchs, A. H. *Phys. Rev. Lett.* **1996**, *76*, 4336.
- (36) Amar, F. G.; Berry, R. S. *J. Chem. Phys.* **1986**, *85*, 5943.
- (37) Smith, R. W. Z. *Phys. D* **1991**, *21*, 57; Román, C. E.; Garzón, I. L. *Z. Phys. D* **1991**, *20*, 163.
- (38) Weerasinghe, A.; Amar, F. G. *J. Chem. Phys.* **1993**, *98*, 4967.
- (39) Rice, O. K.; Ramsperger, H. C. *J. Am. Chem. Soc.* **1928**, *50*, 617; Kassel, L. S. *J. Phys. Chem.* **1928**, *32*, 225.
- (40) Engelking, P. C. *J. Chem. Phys.* **1986**, *85*, 3103; Weisskopf, V. *Phys. Rev.* **1937**, *52*, 295.
- (41) Chesnavitch, W. J.; Bowers, M. T. *J. Chem. Phys.* **1977**, *66*, 2306.
- (42) Parneix, P.; Amar, F. G.; Bréchnignac, P. *Chem. Phys.* **1998**, *239*, 121.
- (43) Calvo, F.; Spiegelmann, F. *J. Chem. Phys.* **2000**, *112*, 2888.
- (44) Cheng, H.-P.; Berry, R. S. *Phys. Rev. A* **1992**, *45*, 7969.
- (45) Doye, J. P. K.; Wales, D. J.; Berry, R. S. *J. Chem. Phys.* **1995**, *103*, 4234.
- (46) Calvo, F. *Phys. Rev. E* **1999**, *60*, 2771.
- (47) Kim, S. G.; Tománek, D. *Phys. Rev. Lett.* **1994**, *72*, 2418.